40-Gb/s PolMux-QPSK transmission using low-voltage modulation and single-ended digital coherent detection

Yong Feng (冯 勇), He Wen (闻 和)*, Hanyi Zhang (张汉一), and Xiaoping Zheng (郑小平)

State Key Laboratory on Integrated Optoelectronics/Tsinghua National Laboratory for Information Science and Technology, Department of Electronic Engineering, Tsinghua University, Beijing 100084, China

**E-mail: wen-he@tsinghua.edu.cn*

Received March 29, 2010

We demonstrate a novel 40-Gb/s transmission system over a 10×101-km standard single mode fiber (SSMF) loop. This system features polarization multiplexed quadrature phase shift keying (PolMux-QPSK), low-voltage modulation of 2-V peak-to-peak signal amplitude, and home-made 90° optical hybrid with single-ended digital coherent detection. Any power amplifers before the modulator and balanced detectors are not used. In the case of low-voltage modulation, coherent detection is much less sensitive to modulator bias offset than delay interferometer-based demodulation.

OCIS codes: 060.0060, 060.1660, 060.5060.

doi: 10.3788/COL20100810.0976.

In recent years, spectral efficient, high-speed optical transmission has been explored using various novel modulations such as differential phase shift keying (DPSK), polarization-multiplexed (PolMux) quadrature phase-shift keying (QPSK)[1−4], PolMux-8PSK[5,6], PolMux-64QAM[7], and optical orthogonal frequency division multiplexing (OFDM)[8]. These modulation methods not only have greatly increased the spectrum efficiency in optical transmission, but also have made the transmitter and receiver increasingly complicated. In this letter, we report a simple 40-Gb/s PolMux-QPSK transmission system over 1000-km standard single mode fiber (SSMF) using home-made polarization diversity 90° hybrids based on fiber devices, single-ended detection, and power-efficient QPSK generation by low-voltage driving signal. Using the novel digital signal processing (DSP) algorithm[6], we find that single-ended coherent detection can be employed in long-haul transmission, which can greatly reduce system cost by replacing more expensive balanced detectors. The frequently used electric amplifiers at the lithium niobate ($LiNbO_3$) modulator are not used, which greatly cuts down the transmitter's power consumption and complexity. Under the same condition, a small direct current (DC) bias offset of Mach-Zehnder modulators (MZMs) can cause large power penalty in the case of delay interferometer detection, but no serious effect in coherent detection.

In the PolMux-QPSK transmission system (Fig. 1), a dual-parallel MZM is used to generate optical QPSK signal. The bias voltages of A, B, and C are carefully adjusted. The in-phase and quadrature (I and Q, respectively) branches are driven by the same 10-Gb/s pseudo-random bit sequence (PRBS, pattern length of 2^{15}–1), and a delay of 51 bits is introduced between them. Electric amplifiers are not used before the modulator, thus the driving signal of data-I and Q have a 2-V peak-to-peak (PP) voltage. Since the incoming signal is small compared with the half-wave voltage ($V_\pi \approx$6 V) of the modulator, it leads to a 22-dB insertion loss. An erbium-doped fiber amplifier (EDFA1) is thus used to raise the signal light power from –18 to ∼3 dBm. After the modulator, the signal light is separated into two copies by a 3-dB coupler and then one path is delayed by a SSMF of about 3 m, causing the data in the two paths to become uncorrelated. Then, the two signals are combined by a polarization beam combiner (PBC). Afterward, the PolMux-QPSK signal circles around the fiber loop. MagLight optical switches 1 and 2 are used in the loop and a MSP430 micro-controller is used to control the switches. The loop contains a 3-dB coupler, a 101-km SSMF, and an optical filter with 0.8-nm bandwidth, which has a total loss of about 30 dB (3+21+6 dB). The light power launched into the 101-km fiber is about –1 dBm. The loop loss is compensated by EDFA2, which has a noise figure of about 5 dB. Meanwhile, the loop dispersion is compensated by a digital finite impulse response (FIR) filter in the receiver instead of a dispersion compensation fiber. In the loop, the optical signal-to-noise ratio (OSNR) of the output light can be calculated according to

$$\mathrm{OSNR} = 58 + P_{\mathrm{out}} - G - \mathrm{NF} - 10\lg N. \qquad (1)$$

The output power from EDFA2 P_{out} is 8 dBm, the total loop loss G=30 dB, and the EDFA noise figure NF=5 dB. After N=10 circles, OSNR is 21 dB.

At the receiver end, a home-made polarization diversity 90° hybrid based on fiber devices[9] is employed to mix signal with the local lightwave emitted from a distributed feedback (DFB) laser with 5-MHz linewidth for single-ended digital coherent detection. The cost-effective 90° hybrid is composed of three fiber couplers and three PBCs with stability longer than 24 h. The complex optical fields $I_x + \mathrm{j}Q_x$ and $I_y + \mathrm{j}Q_y$ in the x and y axes are digitalized and stored through an Agilent real-time sampling scope (DSO81204) with a 20-GS/s sampling rate. The sampled data length is 20 μs, which is limited by the memory depth of the scope. DSP algorithms, including normalized regulation (calibration of the non-ideal feature of the 90° hybrid such as nonorthogonality and inequality of the I and Q branches), chromatic dispersion compensation, polarization demultiplexing, carrier phase

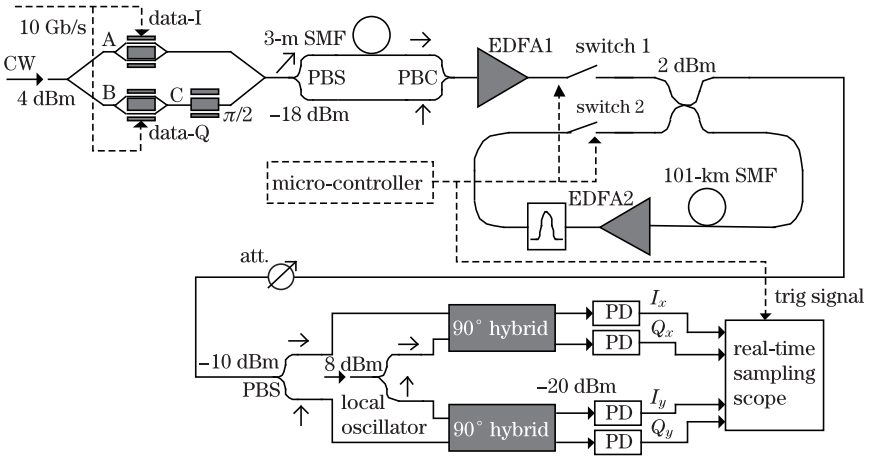

Fig. 1. PolMux-QPSK transmission system with a single-ended polarization diversity-coherent receiver. PBS: polarization beam splitter. PD: photodetector.

estimation, and some other equalizations are then performed offline to retrieve data.

At the receiver, the complex optical field $\begin{bmatrix} E_x & E_y \end{bmatrix}$ of the received signal light is obtained with the help of polarization-diverse optical coherent detection. To separate the polarization multiplexed signals, the inverse Jones matrix $\begin{bmatrix} h_{xx} & h_{xy} \\ h_{yx} & h_{yy} \end{bmatrix}$ of the transmission fiber is calculated using the adaptive constant modulus algorithm (CMA). The offline processing includes chromatic dispersion compensation[10], CMA-based polarization demultiplexing[2] instead of optical demultiplexing[11], and phase noise estimation[3]. The originally transmitted complex signal $\begin{bmatrix} E'_x & E'_y \end{bmatrix}$, contaminated by noise, is calculated to construct a signal constellation diagram, as shown in Fig. 2.

The constellation diagrams in the case of 100-, 500-, and 1000-km transmission are plotted in Fig. 3. In the figures, the shape of the constellation diagram is not a square but a rhombus (originally demodulated constellation diagram). The reason is that the optical phase difference between the two paths of the dual-parallel MZM is not exactly $\pi/2$, which is a serious problem in delay interferometer-based demodulation but less in coherent detection. The left constellation diagrams are for x polarization, while the right ones are for y polarization. We can see that the noise of x polarization is larger. This can be attributed to the weaker power and larger power deviation of x polarization, which experiences a delay line of the SMF fiber. The resulted difference of OSNR between the x and y polarizations increases through the increasing circling number in the gain competition in EDFA (Fig. 3). In a practical coherent system, the x and y polarizations cannot be distinguished because of the symmetrical characteristics of the CMA if the two polarizations are independently modulated. In the experiment, this discrimination is achieved by the fixed time delay between the modulated data on the x and y axes. In a practical polarization multiplexed system, some label bits for channel tracking may be added in the x or y polarization channel to solve this problem.

In the experiment, the small bias offset of the modulator could cause more serious distortion of the signal diagram because we did not use electrical amplifiers to drive the $LiNbO_3$ MZM. However, compared with the delay interferometer-based detection, coherent detection can tolerate this distortion better. In this letter, we compare two detection methods for QPSK signal—delay-interferometer based detection and coherent detection—using the VPI simulation tool. The (normalized) demodulated eye diagram distorted by 5% V_π of bias offset from the NULL point of the MZM modulator is recorded by delay interferometer-based detection with and without drivers (signal amplitude (PP) $\approx$ 8 and 2 V, $V_\pi \approx 6$ V), as shown in Fig. 4.

Apparently, the demodulated signal is seriously affected by the bias offset of the modulator in the case of small signal modulation; the bias offset NULL point breaks up the symmetry of the constellation diagram. In the delay interferometer-based detection, this asymmetry causes a multi-level demodulated signal, which is dependent on the amplitude and phase shift combination of two adjacent symbols. Such condition becomes even more serious in small signal modulation because the symbol

$$\begin{bmatrix} E_x \\ E_y \end{bmatrix} = \begin{bmatrix} I_x + \mathrm{j}Q_x \\ I_y + \mathrm{j}Q_y \end{bmatrix} \xrightarrow{\text{chromatic dispersion compensation}} \begin{bmatrix} E_{x1} \\ E_{y1} \end{bmatrix} = \begin{bmatrix} I_x(n) \otimes h(n) \\ I_y(n) \otimes h(n) \end{bmatrix}$$

$$\xRightarrow{\text{polarization demultiplexing}} \begin{bmatrix} E_{x2} \\ E_{y2} \end{bmatrix} = \begin{bmatrix} h_{xx} & h_{xy} \\ h_{yx} & h_{yy} \end{bmatrix} \begin{bmatrix} E_{x1} \\ E_{y1} \end{bmatrix} \xrightarrow{\text{phase noise estimation and compensation}} \begin{bmatrix} E'_x \\ E'_y \end{bmatrix} = \begin{bmatrix} E_{x2} \times \mathrm{e}^{\mathrm{j}\varphi_{n1}} \\ E_{y2} \times \mathrm{e}^{\mathrm{j}\varphi_{n2}} \end{bmatrix}$$

Fig. 2. Digital algorithm of offline processing.

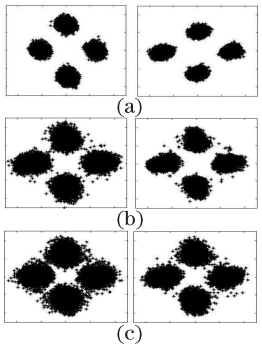

Fig. 3. QPSK constellation diagrams of different transmission distance (a) 100, (b) 500, and (c) 1000 km.

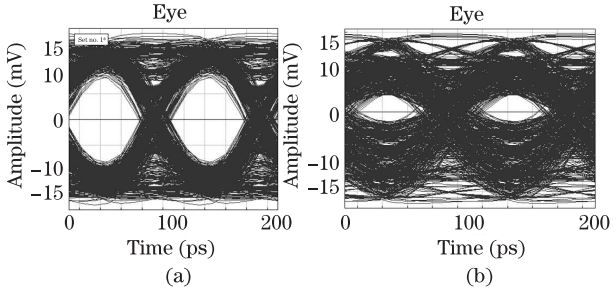

Fig. 4. Eye diagrams based on delay interferometer detection (a) with and (b) without amplifiers.

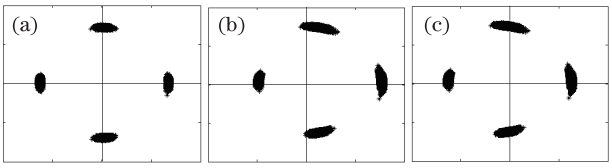

Fig. 5. Constellation diagrams based on coherent detection (a) with amplifiers, (b) without amplifiers, and (c) without amplifiers but compensated by digital signal processing.

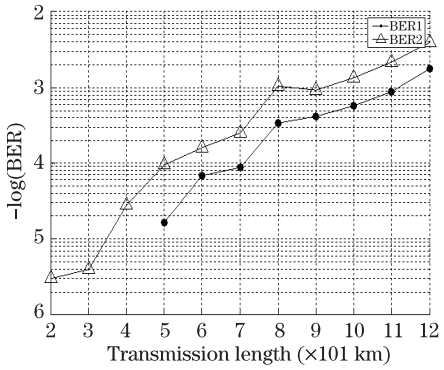

Fig. 6. BER versus transmission distance with (BER2) and without (BER1) digital processing.

magnitude variation is enlarged. In coherent detection, however, this asymmetry causes the constellation diagram to move to a non-zero point that can be easily compensated by DSP, as shown in Fig. 5.

Consequently, in a coherent detection system, low-voltage modulation without driver is applicable because it is robust to the bias offset of a modulator and cost effective by simplifying the transmitter.

The received signal is decoded differentially and the bit error rate (BER) calculated by comparing the decoded bits with the known bit sequence. The BERs versus transmission distance with and without a single-ended noise reduction algorithm[5] are plotted in Fig. 6, in which only the BER of the x polarization is plotted similar to that of the y polarization. In the experiment, the storage depth of the Agilent real-time scope is 4×10^5 samples (20 μs for 20 GS/s sampling rate). Thus the BER is calculated based on 4×10^5 bits, and any BER below 2.5×10^{-6} is unavailable. The single-ended noise reduction algorithm is used to suppress the squared distortion of signal in single-ended detection resulting from the square-law detection of light in the photodiode, which allows larger signal input power. Result shows that this algorithm can reduce about half of the BER and PolMux-QPSK based on single-ended coherent detection can be transmitted over a 1200-km fiber if forward error correction (FEC) is applied in a practical system.

In conclusion, we demonstrate a simple and low-cost 40-Gb/s PolMux-QPSK transmission system that employs low-voltage modulation, home-made fiber-based optical 90° hybrid, and single-ended coherent detection to achieve transmission over 10×101-km SSMF fiber loop with a 30-dB loop loss. Low-voltage modulation is found applicable in a coherent system compared with delay interferometer-based detection because it is robust to the bias offset of a modulator.

This work was supported in part by the National Natural Science Foundation of China (No. 60932004), the "863" Project of China (Nos. 2009AA01Z223 and 2009AA01Z253), and the Open Fund of the Key Laboratory of Information Photonics and Optical Communications (Beijing University of Posts and Telecommunications), Ministry of Education. The authors would like to thank Professor Ping-Tong Ho for his valuable contributions.

References

1. D. van den Borne, S. Jansen, E. Gottwald, E. Schmidt, G. Khoe, and H. de Waardt, in *Proceedings of OFC 2008* OMQ1 (2008).
2. T. Pfau, C. Wördehoff, R. Peveling, S. Ibrahim, S. Hoffmann, O. Adamczyk, S. Bhandare, M. Porrmann, R. Noé, and A. Koslovsky, in *Proceedings of OFC 2008* OTuM3 (2008).
3. D. S. Ly-Gagnon, S. Tsukarnoto, K. Katoh, and K. Kikuchi, J. Lightwave Technol. **24,** 12 (2006).
4. W. Xu, G. Duan, G. Fang, L. Xi, and X. Zhang, Acta Opt. Sin. (in Chinese) **28,** 226 (2008).
5. J. Yu, X. Zhou, M.-F. Huang, Y. Shao, D. Qian, T. Wang, M. Cvijetic, P. Magill, L. Nelson, M. Birk, S. Ten, H. B. Matthew, and S. K. Mishra, in *Proceedings of ECOC 2008* **7,** 27 (2008).
6. X. Zhou, J. Yu, D. Qian, T. Wang, G. Zhang, and P. Magill, J. Lightwave Technol. **27,** 146 (2009).
7. A. Sano, T. Kobayashi, K. Ishihara, H. Masuda, S. Yamamoto, K. Mori, E. Yamazaki, E. Yoshida, Y. Miyamoto, and T. Yamada, in *Proceedings of ECOC 2009* **8,** 1 (2009).
8. W. Shieh, Q. Yang, Y. Ma, W. Shieh, Q. Yang, and Y. Ma, Opt. Express **16,** 6378 (2008).
9. Y. Feng, H. Wen, H. Zhang, and Y. Guo, Chinese J. Lasers (in Chinese) **37,** 471 (2010).
10. E. Ip and J. M. Kahn, J. Lightwave Technol. **25,** 2033 (2007).
11. X. Zhang, G. Fang, X. Zhao, and S. Wang, Acta Opt. Sin. (in Chinese) **29,** 888 (2009).